THE UNIVERSITY OF MICHIGAN
7577-3-Q

Technical Report ECOM-01499-3 June 1966

Azimuth and Elevation Direction Finder Study

Third Quarterly Report

1 March - 31 May 1966

Report No. 3

Contract DA 28-043 AMC-01499(E)
DA Project 5A6 79191 D902 01 04

Prepared by

D. L. Sengupta, J. E. Ferris, G. Hok, R. W. Larson and T. M. Smith

The University of Michigan Radiation Laboratory
Department of Electrical Engineering
Ann Arbor, Michigan

For

United States Army Electronics Command, Fort Monmouth, N. J.

ABSTRACT

Radiation properties of a spherical antenna array are discussed. The array consists of circularly polarized antenna elements arranged according to a predetermined fashion on a spherical surface. The variation of the radiation patterns, directivity and the half-power beamwidths of the patterns with the change of different parameters of the array are discussed. A simple approximate (but useful) expression is given which can be used to analyze the patterns produced by a spherical array. Subsidiary lobes in the pattern produced by circular arrays of isotropic elements are discussed.

A technique of correlation processing of the output data from each antenna element of the array for direction finding purposes is described.

Experimental patterns produced by a flat spiral antenna are given.

FOREWORD

This report was prepared by The University of Michigan Radiation Laboratory of the Department of Electrical Engineering under United States Army Electronics Command Contract No. DA 28-043 AMC-01499(E). This contract was initiated under United States Army Project No. 5A6 79191 D902 01 04 "Azimuth and Elevation Direction Finder Study". The work is administered under the direction of the Electronics Warfare Division, Advanced Techniques Branch at Fort Monmouth, New Jersey. Mr. S. Stiber is the Project Manager and Mr. E. Ivone is the Contract Monitor.

The material reported herein represents the results of the preliminary investigation into the study of the feasibility of designing a broadband circularly polarized direction finder antenna with hemispherical coverage.

TABLE OF CONTENTS

LIST OF ILLUSTRATIONS

I
INTRODUCTION

This is the third report on a study to determine the possibility of developing a broadband VHF azimuth and elevation direction finder. The first report (Sengupta, et al, 1965) discussed theoretically the possibility of using an antenna array consisting of circularly polarized antenna elements placed on the surface of a sphere. The second report (Sengupta, et al, 1966) discussed the different aspects of the radiation characteristics of such an array. It also discussed the application of a signal processing method which eliminates the use of a phase shifter for each antenna element. The plan of the present report is as follows.

The radiation patterns produced by a spherical array with a special type of element distribution were discussed in our second report. Chapter II of the present report discusses the results obtained when a slightly modified element distribution is used. The motivation of changing the previous element distribution was to ascertain whether it is possible to make the patterns more symmetric than was obtainable before. The effects of varying the activated area of the spherical surface and also of the beam steering on the patterns are discussed. The variation of the directivity of the array as a function of frequency and activated area is discussed. A simple expression is given which under some special conditions can be used to analyze the main beam and first sidelobe of the pattern produced by a spherical array.

Chapter III discusses the subsidiary lobes in the patterns produced by a circular array of isotropic sources under different situations.

The arrays described in Chapters II and III are for conventional phased arrays. Their desired performance requires a broadband phase shifting device for each antenna element of the array. Chapter IV describes an alternative approach which uses the technique of correlation processing of the output data from each antenna element. This eliminates the use of phase shifters which may be an

advantage in some cases. The possibility of using this method to direction finding with a spherical antenna array is described in detail. The basic system requirements and the implementation of such a procedure are also discussed.

Chapter V gives the results of experimental investigation of the properties of flat spiral antennas.

II

RADIATION CHARACTERISTICS OF THE SPHERICAL ARRAY

The radiation properties of a spherical antenna array with a special type element distribution obtained from a study of the icosahedron geometry were discussed in the previous report (Sengupta, et al, 1966). The present chapter discusses the results obtained when a slightly modified element distribution is used. The element distribution has been modified in order to ascertain whether it is possible to make the patterns more symmetric in the region beyond the second sidelobe. This attempt resulted in no appreciable changes in the patterns as compared to those reported earlier. The effects of varying the extent of the activated area of the spherical surface on the patterns are discussed. More results are reported on the directivity of the antenna array. Finally, a simple approximate expression is given which can be used under some special conditions to analyze the radiation patterns produced by a spherical antenna array.

2.1 Theoretical Expression for the Radiation Pattern

The far zone electric field produced by a spherical array of circularly polarized antenna elements may be written as

$$\tilde{E}(\theta, \phi) = -(\hat{e}_\theta - i\hat{e}_\phi)A(\theta, \phi) , \qquad (2.1)$$

where

θ, ϕ are the spherical coordinates of the observation point,

$\hat{e}_\theta, \hat{e}_\phi$ are the unit vectors in θ and ϕ directions, respectively,

$A(\theta, \phi)$ may be looked upon as the pattern factor of the spherical array and is given by the following,

$$A(\theta,\phi)=\sum_{n=-6}^{6}\sum_{m=o}^{M(n)}\delta_{nm}\psi_{nm}e^{i\left[ka(\psi_{mn}-\Delta_{nm})-(\xi_{nm}-\eta_{nm})\right]}, \qquad (2.2)$$

where

$$\psi_{nm}=\sin\alpha_n\sin\theta\cos(\phi-\beta_{nm})+\cos\alpha_n\cos\theta\,, \qquad (2.3)$$

$$\Delta_{nm}=\psi_{nm}(\theta_o,\phi_o)=\sin\alpha_n\sin\theta_o\cos(\phi_o-\beta_{nm})+\cos\alpha_o\cos\theta_o, \qquad (2.4)$$

$$\xi_{nm}=\tan^{-1}\left[\frac{(\cos\alpha_n+\cos\theta)\sin(\phi-\beta_{nm})}{\sin\alpha_n\sin\theta+(\cos\theta\cos\alpha_n+1)\cos(\phi-\beta_{nm})}\right], \qquad (2.5)$$

$$\eta_{nm}=\xi_{nm}(\theta_o,\phi_o)=\tan^{-1}\left[\frac{(\cos\alpha_n+\cos\theta_o)\sin(\phi_o-\beta_{nm})}{\sin\alpha_n\sin\theta_o+(\cos\theta_o\cos\alpha_n+1)\cos(\phi_o-\beta_{nm})}\right], \qquad (2.6)$$

δ_{nm} is a conditional on-off switch governed by ψ_{nm} and Δ_{nm},

α_n, β_{nm} are the coordinates of an antenna element on the spherical surface,

θ_o, ϕ_o give the direction of the pattern maximum,

k is the wave number, and

a is the radius of the sphere.

The above expressions were derived and discussed in our Second Quarterly Report. It assumes that each antenna element of the array produces circularly polarized radiation.

2.2 Element Distribution

The modified element arrangement is given by the following relations.

$$\alpha_n = 90^o - n\,15^o \quad , \tag{2.7}$$

$$\left.\begin{aligned}
&\beta_{nm} = 72^o m/6 - |n| \quad , && n = 5, 4, 3, 2 \\
&\beta_{nm} = \frac{72^o m}{6-|n|} + 180^o , && n = -5, -4, -3, -2 \\
&\beta_{nm} = 0^o \quad , && n = \pm 6 \\
&\beta_{nm} = \beta_{2m} + 9^o , && n = \pm 1 \\
&\beta_{0m} = \beta_{\beta m} \quad , && n = 0
\end{aligned}\right\} \quad . \tag{2.8}$$

In this arrangement there are 162 elements which is 15 less than in the earlier element arrangement.

With the aid of (2.7) and (2.8) the upper limit of the m summing index M(n) in (2.2) is found to be

$$M(n) = 5(6 - |n|) - 1, \quad \text{for } n = \pm 5, \pm 4, \pm 3, \pm 2,$$
$$M(6) = 0,$$
$$M(0) = M(1) = M(2) \quad .$$

For an activated distribution centered at θ_o, ϕ_o and of size $2\alpha_o$, the on-off condition switch δ_{nm} is

$$\delta_{nm} = \begin{cases} 1 \ , \ \text{if } \Delta_{nm} > \cos\alpha_o \text{ and } \psi_{nm} \geq 0 \\ 0, \ \text{otherwise} \end{cases} \quad . \tag{2.9}$$

In eq. (2.9) $\psi_{nm} \geq 0$ means physically that only those elements which are visible from point (θ, ϕ) contribute to the sum in (2.2). The statement $\Delta_{nm} \geq \cos \alpha_o$ means that only those elements which lie within α_o degrees of the point (θ_o, ϕ_o) contribute to (2.2). ψ_{nm} and Δ_{nm} are defined in (2.3) and (2.4). The following Table II-1 gives the number of active elements for three values of α_o when $\theta_o = 0^o$.

TABLE II-1

α_o	$\Delta_{nm}(\theta_o=0^o, \phi_o=90^o)$	No. Active Elements
75^o	> .00	71
45^o	> .07	31
30^o	> .86	16

As θ_o and ϕ_o change, the number of active elements may vary by as much as 10 per cent for a fixed value of α_o. This fluctuation in the number of active elements is due to the variation of the element distribution as θ_o and ϕ_o vary.

It should be mentioned that there is an approximate relationship between a/λ and the average spacing s between the adjacent elements on the surface of the sphere. For the present icosahedron distribution most of the elements are situated 15^o apart and the average element spacing is given by

$$s \approx 0.30\, a \quad . \tag{2.10}$$

Thus, when $a/\lambda = 1.5$, $s = 0.45\lambda$ and when $a/\lambda = 8.0$, $s = 2.4\lambda$. The exact value of s changes slightly over the surface of the sphere for any fixed value of a/λ.

2.3 Radiation Patterns

Radiation patterns obtained numerically from eq. (2.2) with element distribution given by (2.7) and (2.8) are discussed in this section. Results are given only for the patterns in the polar cut plane. This plane always passes through $(\theta - \theta_o) = 0$ and

is determined by the following parameters.

$$\phi = \phi_0, \quad \theta = \theta_0 + p\Delta\theta, \quad p = 0, 1, 2, \ldots, 360^0/\Delta\theta \quad , \tag{2.11}$$

where $\Delta\theta$ is chosen to be small compared to the pattern fluctuations. The expression for the power pattern normalized with respect to the pattern peak is $|A(\theta, \phi_0)|^2 / |A(\theta_0, \phi_0)|^2$.

Figure 2-1 shows how the pattern changes as the activated region is varied from $\alpha_0 = 75^0$ to $\alpha_0 = 30^0$. As expected, it can be seen from Fig. 2-1 that the main beam broadens with corresponding reduction of the first sidelobe as the activated area is reduced. Since for $a/\lambda = 3.0$, $s = 0.9\lambda$, subsidiary lobes appear in the pattern. These lobes are not of very high amplitude in this particular case. However, for larger a/λ the subsidiary lobes become greater in magnitude as α_0 decreases from 75^0. For $a/\lambda = 8.0$ and $\alpha_0 = 30^0$, the subsidiary lobe has been found to have amplitudes as high as -3 db. In the case of $\alpha_0 = 75^0$ for large spacing between the elements, subsidiary lobes appear in the pattern but they are never so high.

Figure 2-2 shows the effect of beam steering on the pattern. The patterns shown are for the case with $a/\lambda = 3.0$, $\alpha_0 = 45^0$ when the beam is steered over a hemisphere. As the beam is steered the main beam stays approximately constant and the first two sidelobes remain almost symmetric although their levels are found to fluctuate with more and more steering. The subsidiary lobe amplitudes also tend to fluctuate with steering. For $\theta_0 = 35^0$ the subsidiary lobe amplitude takes on a value as high as -12 db compared to the peak of the main beam.

The effects of changing a/λ (i.e. the element spacing s) on the pattern are shown in Fig. 2-3. As expected with increase of a/λ the lobes in the pattern become narrower and the subsidiary lobes increase both in amplitude and number. A short description of the subsidiary lobes in the patterns of a spherical array is

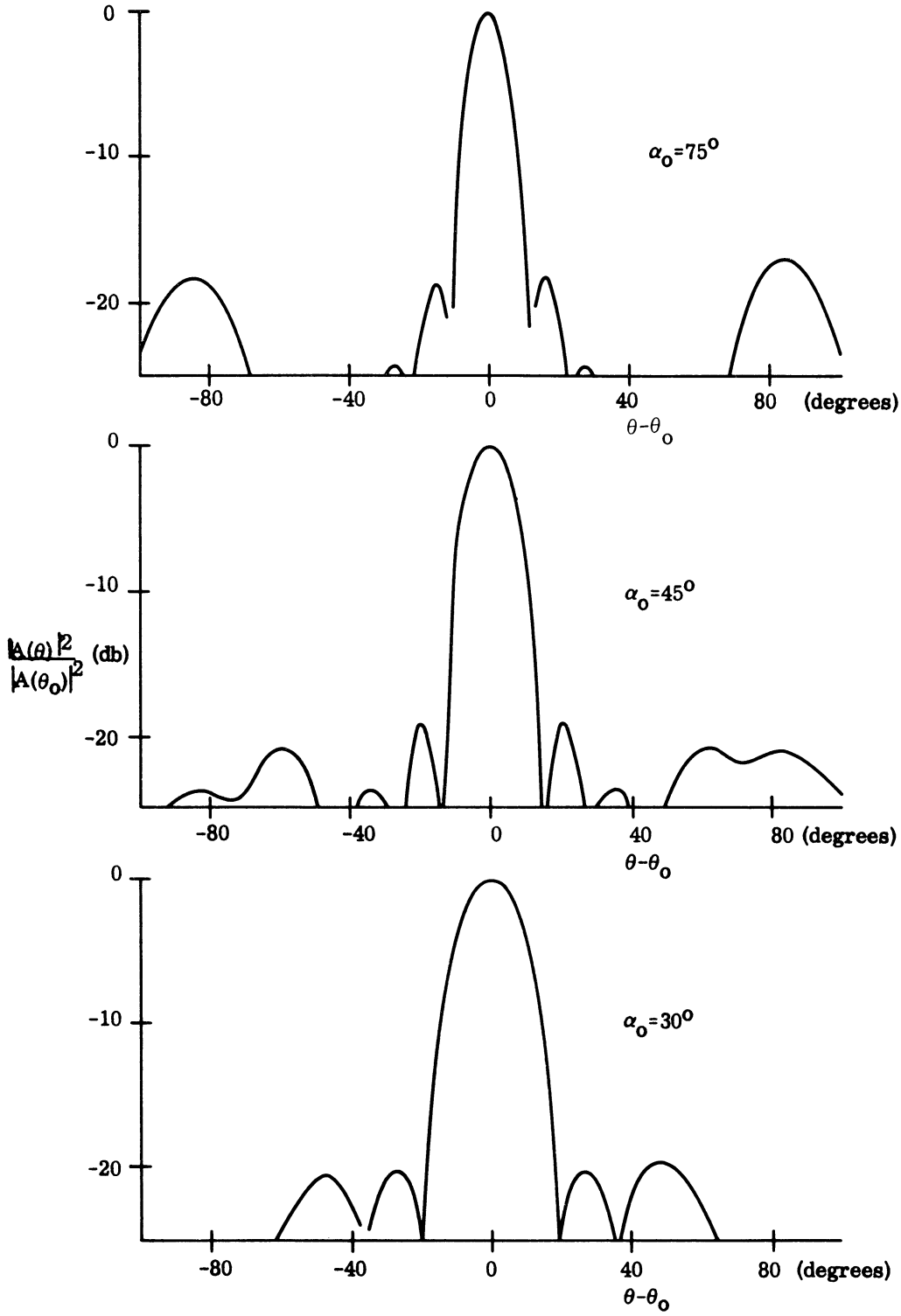

FIG. 2-1: EFFECTS OF VARIATION OF α_o ON RADIATION PATTERNS. a/λ=3.0, θ_o=0°, ϕ_o=90°.

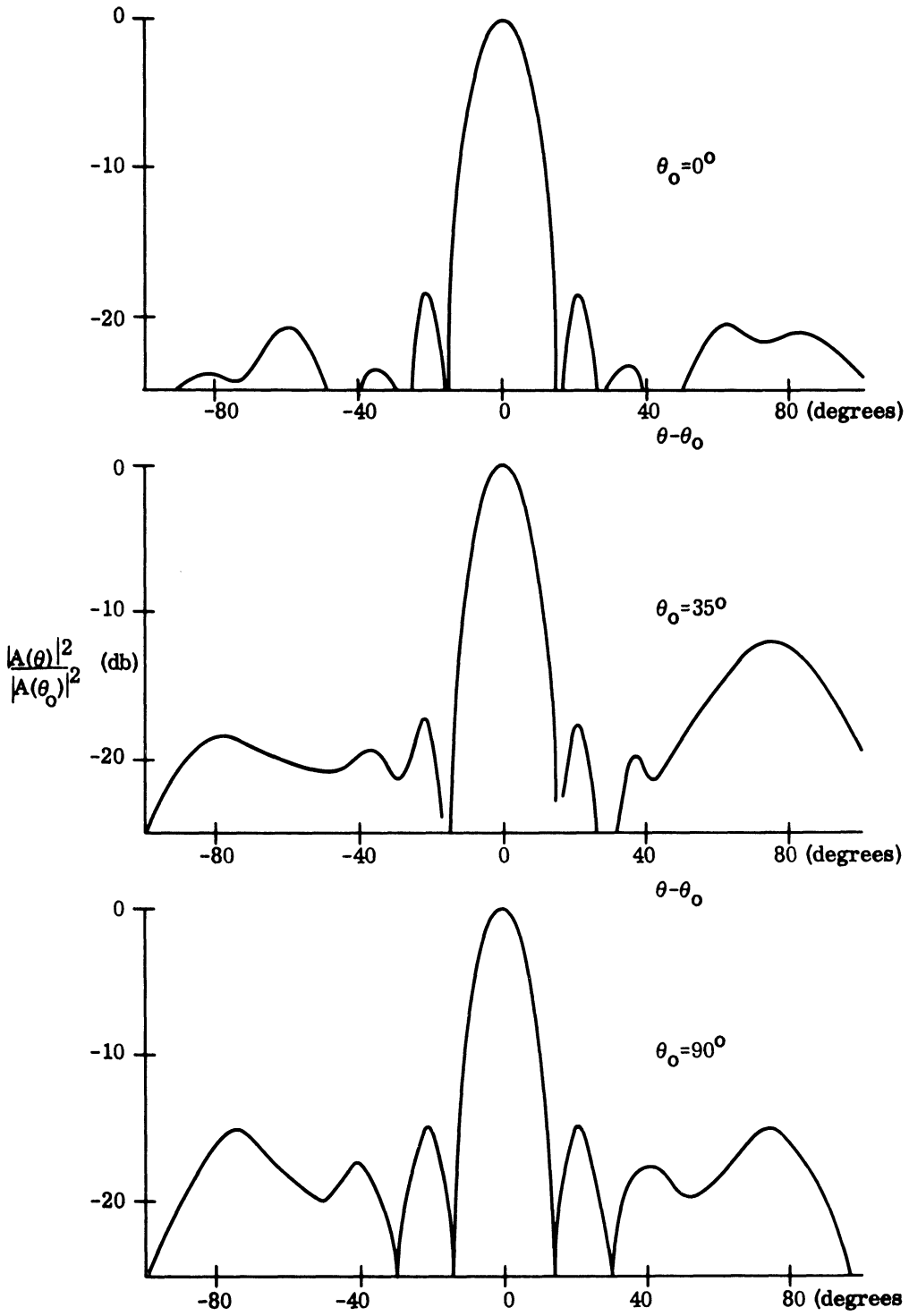

FIG. 2-2: RADIATION PATTERN VARIATION WITH BEAM STEERING.
a/λ=3.0, α_o=45°, ϕ_o= 90°

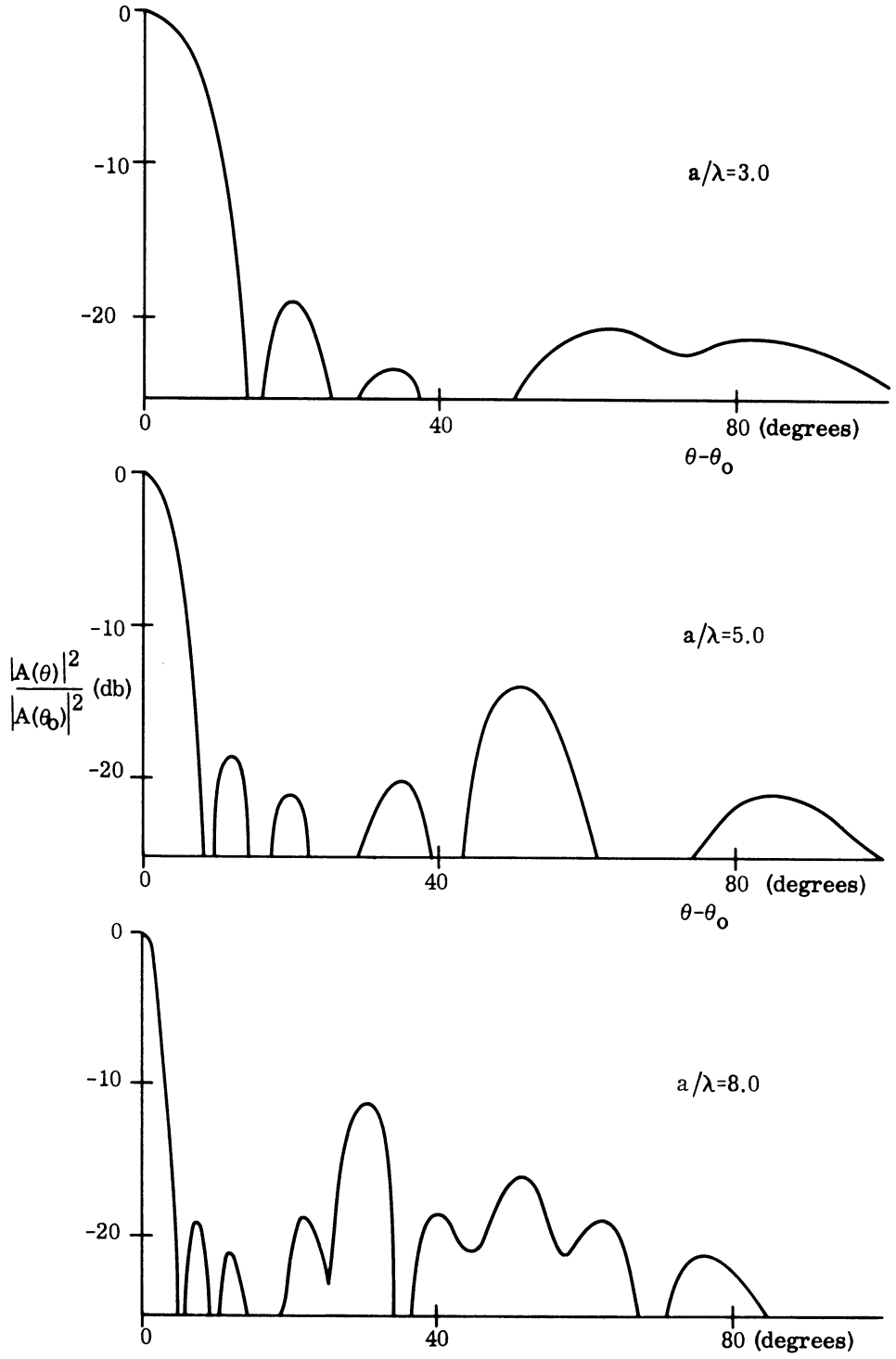

FIG. 2-3: RADIATION PATTERNS FOR VARIATION IN a/λ.
α_o=45°, θ_o=0°, ϕ=90°.

appropriate here. In the next chapter subsidiary lobes in the patterns produced by a circular array of isotropic sources are discussed. There it will be found that for element spacing $s > \lambda/2$ subsidiary lobes appear in the pattern. The amplitude and location of these lobes depends on the number of elements used and the spacing between them. The amplitudes, in general, fluctuate in value as the spacing s is increased. However, in no case do they achieve values equal to the maximum value of the pattern. The behavior of the subsidiary lobes in the case of the spherical array will be similar although, in general, the amplitudes of these lobes will be much reduced due to the spherical distribution of elements.

2.4 Directivity

The directivity of the antenna array is calculated numerically using the relation

$$D = \frac{2\,|A(\theta_0)|^2}{\Delta\theta \sum_{\theta=0^o}^{180^o} |A(\theta)|^2 \sin\theta} \qquad (2.12)$$

where $\Delta\theta$ is chosen to be small compared to the pattern fluctuations. Figure 2-4 shows the numerically computed directivity D as a function of a/λ with α_0 as the parameter.

Over a considerable value of a/λ the directivity for $\alpha_0=45^o$ is larger than for $\alpha_0=75^o$. Ordinarily, one would expect the arrangement with more elements ($\alpha_0=75^o$) to produce a greater directivity. This apparent discrepancy can be attributed to the subsidiary lobes. After examining many patterns in the region where the directivity for $\alpha_0=45^o$ is greater than for $\alpha_0=75^o$, it was found that the subsidiary lobes for $\alpha_0=75^o$ occurred at values of θ which weighted them more in eq. (2.12). The subsidiary lobes seriously affect the directivity of a pattern.

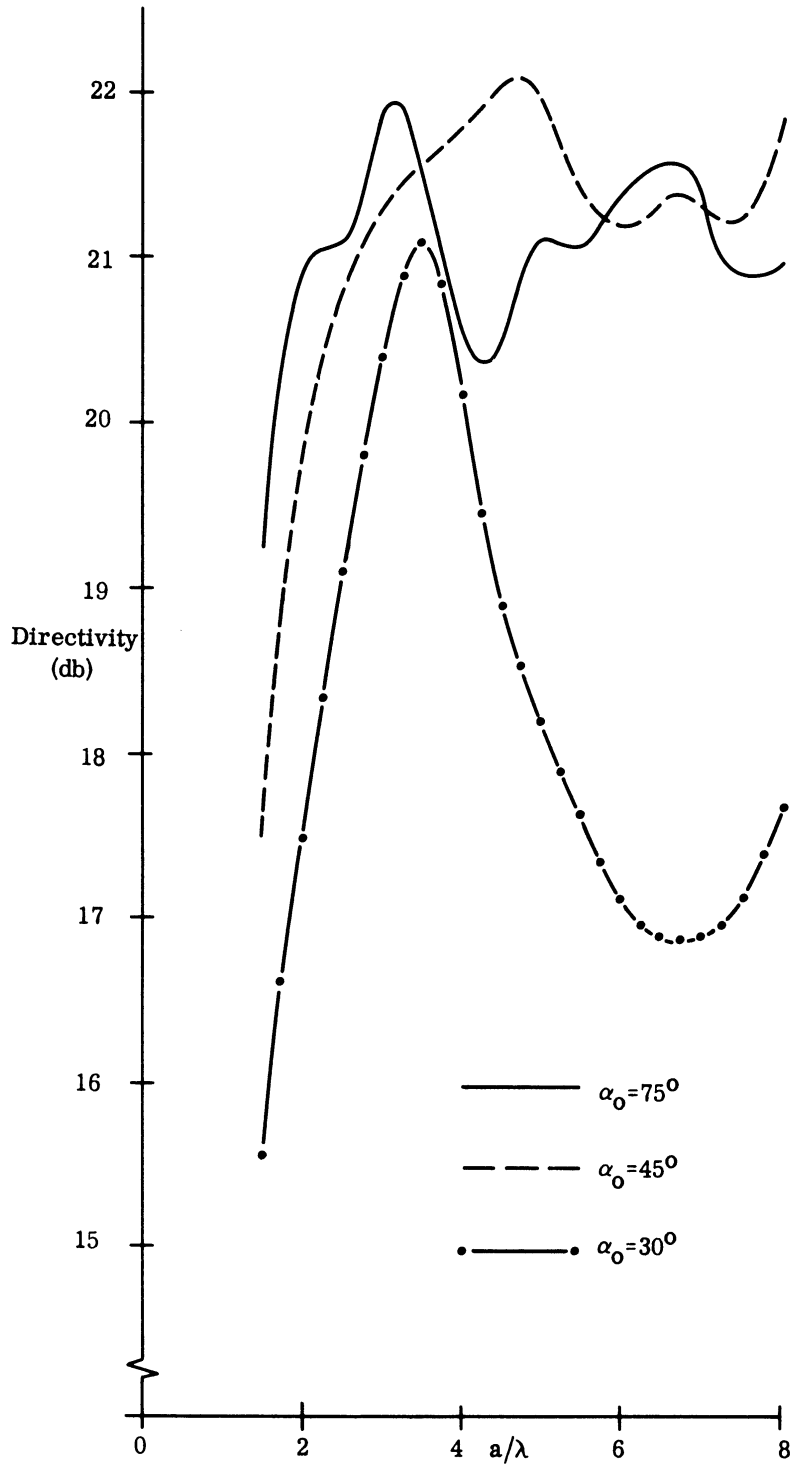

FIG. 2-4: DIRECTIVITY AS A FUNCTION OF a/λ.
θ_o=0°, ϕ_o=90°.

From an economic point of view it seems that $\alpha_0=45^o$ is superior to $\alpha_0=75^o$ since $\alpha_0=45^o$ has only 31 elements as compared to 71 elements for the 75^o case. One disadvantage to the $\alpha_0=45^o$ arrangement is that typically the magnitude of the subsidiary lobes are greater than for $\alpha_0=75^o$.

2.5 Half-power Beamwidth

The half-power beamwidth $\Theta_{1/2}$ of the pattern is shown in Fig. 2-5 as a function of a/λ for different values of activated area. These curves have been obtained numerically from eq. (2.2). The accuracy of the results in Fig. 2-5 is of the order of $\pm 0.5^o$. It is not possible to give an analytic expression for $\Theta_{1/2}$ from a study of (2.2). However, from a study of the numerically computed patterns the following empirical relation has been derived for the half-power beamwidth and of the patterns.

$$\Theta_{1/2} = \kappa \cdot \lambda/a \,, \tag{2.13}$$

where

$\kappa = 0.98$, for $\alpha_0 = 75^o$

$\kappa = 0.70$, for $\alpha_0 = 45^o$

$\kappa = 0.55$ for $\alpha_0 = 30^o$.

In the next section we discuss an approximate expression which can predict the half-power beamwidth of the pattern under some restrictive conditions.

2.6 An Approximate Expression

It can be shown (Smith, 1966) that the main beam and the first sidelobe of the pattern produced by a spherical antenna array of angular dimension α_0 may be approximated by the following expression.

$$\frac{A(\theta)}{A(\theta_0)} = 2\,\frac{J_1(ka \sin\alpha_0 \sin\theta)}{(ka \sin\alpha_0 \sin\theta)} \,, \tag{2.14}$$

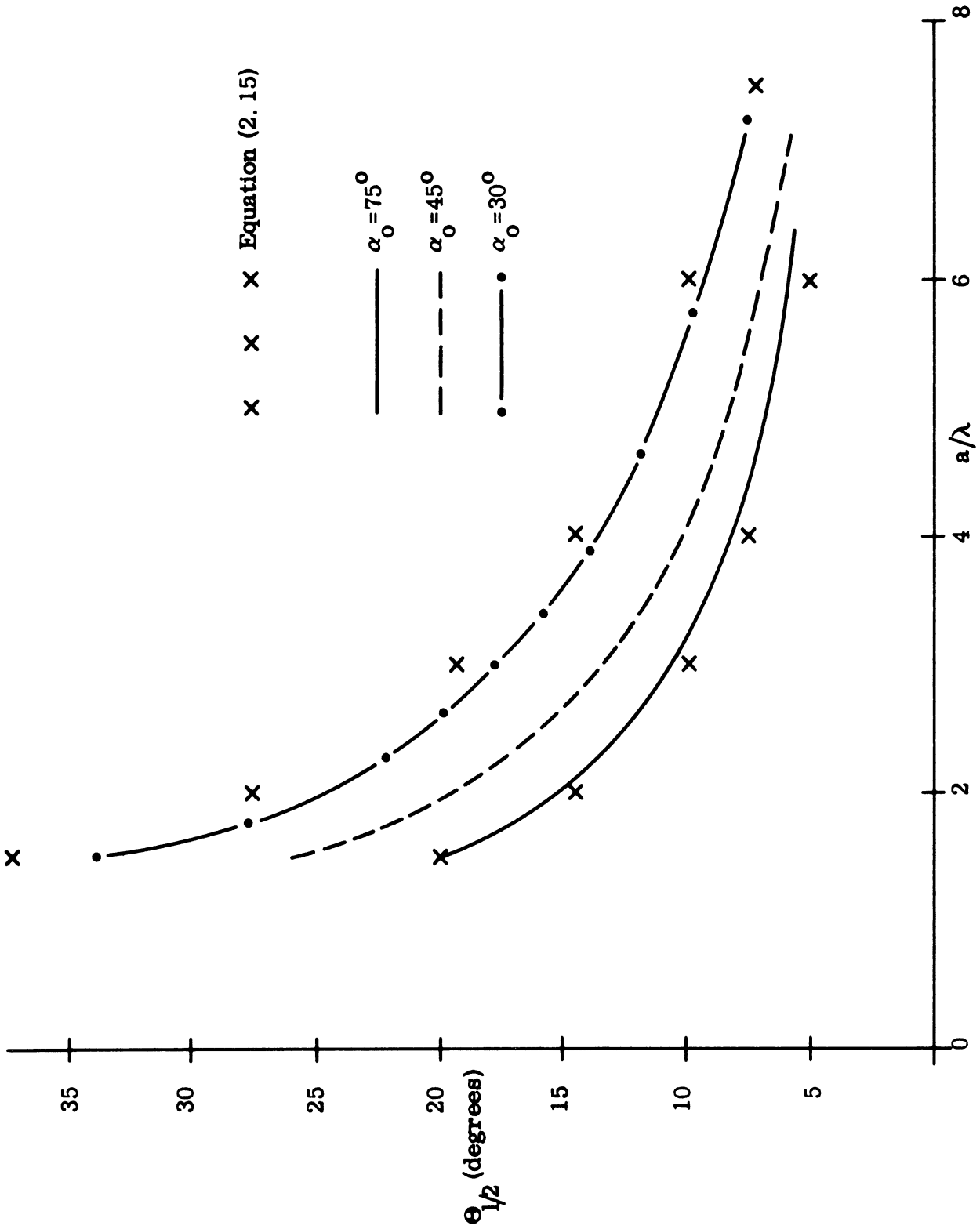

FIG. 2-5: HALF-POWER BEAMWIDTH AS A FUNCTION OF a/λ.

where J_1 is the usual notation for the Bessel function of order unity. The half-power beamwidth predicted by (2.14) is given by

$$\Theta_{1/2} = 2 \sin^{-1}\left[\frac{0.258}{ka \sin\alpha_o}\right] . \qquad (2.15)$$

The half-power points corresponding to α_o=90° and 30° for various values of a/λ are calculated from (2.15) and these are also plotted in Fig. 2-5 for comparison. Except at the point $a/\lambda = 1.5$, α_o=30° where there is a +6° error, eq. (2.15) in general agrees with the results of numerical computation in Fig. 2-5 to within 1.0°. Hence although the approximations involved in (2.14) are crude it may be found to be useful in roughly explaining the patterns produced by a phase directed spherical antenna array. It is interesting to observe that eq. (2.14) is the pattern produced by a uniformly illuminated circular aperture of radius $a \sin\alpha_o$ (Silver, 1949).

III

SUBSIDIARY LOBES IN THE PATTERNS OF CIRCULAR ARRAYS

The pattern produced by a circular array of isotropic elements has been discussed in the last quarterly report (Sengupta, et al, 1966). The case when the array consists of even numbers of elements was discussed in detail. In the following sections results are given for an array with even numbers of elements. The characteristics of the array with odd numbers of elements are also discussed. The discussion is restricted to the pattern produced in the plane of the array.

3.1 Pattern Expressions

The array is assumed to consist of isotropic elements, placed uniformly along the circumference of a circle. The elements are excited with equal amplitude but their phases are so adjusted that the resulting pattern has a maximum along a certain direction. Let us assume that the number of element used is M and the radius of the array is a . The plane of the array is in the xy-plane of a Cartesian coordinate system xyz, with the origin at the center of the circular array, which is also taken to be the phase center of the array. If the elements are phased so that there is a maximum along $\phi=0^{o}$ (x-axis), then it can be shown that the normalized pattern produced in the plane of the array, i. e. in the xy-plane, is given by

$$A_e(\phi)=J_o(\rho)+2\sum_{n=1}^{\infty} J_{Mn}(\rho)\cos\left(\frac{Mn\phi}{2}\right), \quad \text{when M is even,} \qquad (3.1)$$

$$\left[A_o(\phi)\right]^2=\left[J_o(\rho)+2\sum_{n=1}^{\infty} J_{2Mn}(\rho)\cos Mn\phi\right]^2+\left[2\sum_{n=0}^{\infty} J_{M(2n+1)}(\rho)\sin\frac{M(2n+1)}{2}\phi\right]^2$$

when M is odd, (3.2)

where

$$\rho = 2ka \sin \phi/2 \tag{3.3}$$

$$k = \frac{2\pi}{\lambda} = \text{propagation constant}.$$

J's are the usual notations for the Bessel functions of the first kind.

The exact expression for the pattern in the plane of the array for both M even and odd is,

$$A(\phi) = \frac{1}{M} \sum_{m=1}^{M} e^{ika\left\{\cos\left(\frac{2\pi}{M}m - \phi\right) - \cos\frac{2\pi}{M}m\right\}} . \tag{3.4}$$

If $M \gg 2ka$ which means that the spacing between the adjacent elements $s \ll \lambda/2$ then both equations (3.1) and (3.2) may be approximated as follows:

$$A_e(\phi) = A_o(\phi) \approx J_o(\rho) . \tag{3.5}$$

Thus in this case the pattern is independent of the number of elements used and the pattern expression (3.5) is much simpler than the exact expression given by (3.4).

As was discussed in the Second Quarterly Report, eqs. (3.1) and (3.2) predict that when $s > \lambda/2$ (i.e. $M \geq 2ka$) subsidiary lobes appear in the pattern which cannot be explained by the simple expression (3.5). It can be seen now that when $s > \lambda/2$ the pattern is no longer independent of the number of elements. However, the main beam and the first few sidelobes can still be explained by (3.5). The subsidiary lobes will be determined by the higher order terms in (3.1) and (3.2). Moreover, the behavior of these lobes will depend on whether the number of elements used is even or odd. In order to compare the two cases let us consider a simple case when $M < 2ka < 2M$. Under this assumption we may write (3.1) and (3.2) as follows:

$$A_e(\phi) \simeq J_o(\rho) + 2J_M(\rho)\cos\frac{M\phi}{2} \quad , \qquad M \text{ even} , \tag{3.6}$$

$$\left|A_o(\phi)\right| \simeq \left[J_o^2(\rho) + 4J_M^2(\rho)\sin^2\frac{M\phi}{2}\right]^{1/2} \quad , \qquad M \text{ odd} . \tag{3.7}$$

It can be seen from (3.6) and (3.7) that for the same value of ka and even M, the subsidiary lobe amplitudes with (M-1) elements will be less than the case with M elements. From this simple example one can generalize that in a circular array of isotropic elements it is preferable to use odd numbers of elements so that the subsidiary lobe amplitudes may not be too high.

3.2 Subsidiary Lobes: M even.

In the Second Quarterly Report we developed an approximate method to predict the subsidiary lobes in the pattern produced by a circular array. In particular we discussed in detail the case with ka = 4π and M = 8. There we defined the subsidiary lobe as one with an amplitude larger than the first side lobe corresponding to $J_o(2ka \sin \phi/2)$ i.e. > 0.4028. Approximately the first subsidiary lobe will appear in the region of ϕ given by

$$2ka \sin \phi/2 = M + 1.0188 \left(\frac{M}{2}\right)^{1/3} . \tag{3.8}$$

At the value of ϕ given by (3.8) the coefficient $J_M(\rho)$ in eq. (3.6) takes on its maximum value. It should be mentioned here that $A_e(\phi)$ will have a strong subsidiary lobe at the angle ϕ given by (3.8) only when the two terms in (3.6) are in phase. The maximum of the Bessel function of higher order may be directly obtained from the tables. If the table is not available one can use the following procedure.

$$J_M(2ka \sin \phi/2) \approx \frac{Ai\left[\dfrac{M - 2ka \sin \phi/2}{(M/2)^{1/3}}\right]}{(M/2)^{1/3}} \quad , \tag{3.9}$$

for 2ka sin $\phi/2$ near M. Ai is the Airy function. The first maximum of the Airy function is: Ai(-1.0188) = 0.535. Using the above procedure we have calculated the position and amplitudes of the first subsidiary lobes in the pattern produced by the circular case with ka = 4π and various values of M. The results of the approximate analysis along with those obtained from the exact expression (3.4) are shown in Table III-1.

TABLE III-1

M	Position	Amplitude (approx.)	Amplitude (exact)
8	45°	-0.8867	-0.8759
12	66° 54'	+0.6534	+0.6048
14	78° 50'	-0.7179	-0.6963
16	91° 46'	+0.5060	+0.4828
20	124° 2'	-0.5889	-0.5978

Equation (3.4) has been computed for various values of ka and even M. Table III-2 gives the positions and amplitudes of the subsidiary lobes in the pattern for ka = 4π and various even values of M.

TABLE III-2

	Positions and Amplitudes of Subsidiary Lobes					
M	Position	Amplitude	Position	Amplitude	Position	Amplitude
10	64°	0.512	80°	0.508	130°	0.646
12	64°	0.722	96°	0.448	-	-
14	80°	0.697	-	-	150°	0.417
16	92°	0.504	-	-	134°	0.536
20	108°	0.501	-	-	126°	0.641
24	180°	0.522	-	-	-	-

3.3 Subsidiary Lobes: M odd.

Following the same approximate procedure the first subsidiary lobes may be investigated by using (3.7). We do not discuss the procedure here. Patterns have been calculated for arrays with odd numbers of elements using (3.4). Table III-3 shows the subsidiary lobe positions and amplitudes for an array with ka = 4π and various odd values of M.

TABLE III-3

	Positions and Amplitudes of Subsidiary Lobes					
M	Position	Amplitude	Position	Amplitude	Position	Amplitude
9	52^o	0.527	100^o	0.482	180^o	0.485
13	70^o	0.549	-	-	-	-
15	84^o	0.562	-	-	-	-
19	104^o	0.456	122^o	0.468	-	-

It can be seen from Tables III-2 and III-3 that for the same value of ka the subsidiary lobes are less pronounced for odd values of M than in the case with even values of M.

IV

CORRELATION PROCESSING OF THE OUTPUT DATA

4.1 Introduction

4.1.1 Alternative Approaches

The task of the data processing system is to analyze the signals induced in all the elements of the antenna array and, from the results, compute the angle of incidence of each arriving wave or wave train.

This may be accomplished by controlling the directional pattern of the array with variable phase-shifting networks, or by the correlation data processing techniques proposed in the Second Quarterly Report and described below. Since we find the latter scheme to be practical for the data rates which a direction finder must be able to handle in order to satisfy the specifications proposed in the guidelines for the present project, we shall in subsequent sections of this chapter discuss the requirements and implementation of such a procedure.

4.1.2 Basic Equations for Correlation Processing.

The Second Quarterly Report outlined the correlation processing technique for determining both elevation and azimuthal arrival directions for signals over a wide range of frequencies. The basic idea of this approach is to compare (or 'correlate') the actual signals induced at the elements of an array with the signals which would be induced if the source were located at a known position and frequency. The frequency and direction of arrival can then be estimated or calculated from the resulting correlation display.

The correlation is defined (from the previous Quarterly with a slight change in nomenclature) as:

$$R = \sum_{nm} R_{nm} = \sum_{nm} \frac{1}{T} \int_{T} x_{nm}(t)\, s^{*}_{nm}(t)\, dt \quad . \qquad (4.1)$$

There will be an unknown, and generally varying, phase difference between the incident ($x_{nm}(t)$ and reference (s_{nm}) waves. It is, therefore, desirable to define a conjugate correlation $\bar{R}$, utilizing a 90^o phase difference for the reference wave, $s_{nm}(t+\pi/2\omega)$. As discussed in the previous Quarterly Report, it is also possible to define R and $\bar{R}$ in terms of orthogonal, real components of x_{nm} and s^*_{nm}:

$$\left.\begin{aligned} R_{nm}&=2(X_{nm}P_{nm}+Y_{nm}Q_{nm}) \\ \bar{R}_{nm}&=2(X_{nm}Q_{nm}-Y_{nm}P_{nm}) \end{aligned}\right\} , \tag{4.2}$$

where the various notations are as described in the previous report.

In the preceding brief description of the correlation process, the nature of the element and reference signals has not been discussed. For reasons detailed previously, it is appropriate to consider an array of spiral antennas on a spherical surface. It has already been shown (eq. (2.9) of the Second Quarterly) that the (unphased) contribution of the signal received from the nm'th spiral antenna at the location (α_n, β_{nm}) in the direction θ_r, ϕ_s , and for wave number $k_q=\omega_q/c$, would then be:

$$E_{nm}(\omega_q, \theta_r, \phi_s)=\psi_{nm}(\theta_r, \phi_s)e^{j\Phi_{nm}(\omega_q, \theta_r, \phi_s)} , \tag{4.3}$$

where ψ_{nm} and Φ_{nm} are given by:

$$\psi_{nm}(\theta_r, \phi_s)=\cos\theta_r\cos\alpha_n+\sin\theta_r\sin\alpha_n\cos(\phi_s-\beta_{nm}) \tag{4.4}$$

$$\Phi_{nm}(\omega_q, \theta_r, \phi_s)=k_q\, a\psi_{nm}(\theta_r, \phi_s)+\xi_{nm}(\theta_r, \phi_s) \tag{4.5}$$

$$\xi_{nm}(\theta_r, \phi_s)=\tan^{-1}\left[\frac{(\cos\alpha_n+\cos\theta_r)\sin(\phi_s-\beta_{nm})}{\sin\alpha_n\sin\theta_r+(\cos\theta_r\cos\alpha_n+1)\cos(\phi_s-\beta_{nm})}\right] \tag{4.6}$$

Equations (4.4) and (4.6) are similar to Eqs. (2.3) and (2.5) of the Second Quarterly Report,with a slight change in notations.

Using reciprocity, it can be seen that the signal received by that element would be the same and therefore in the present nomenclature (taking the conjugate):

$$s^*_{nm}(\omega_q, \theta_r, \phi_s) = \psi_{nm}(\theta_r, \phi_s) e^{-j\Phi_{nm}(\omega_q, \theta_r, \phi_s)} \quad . \tag{4.7}$$

The signal received from the source at $(\theta_o, \phi_o, \omega_o)$ is similarly

$$x_{nm}(\omega_o, \theta_o, \phi_o) = \psi_{nm}(\theta_o, \phi_o) e^{j\Phi_{nm}(\omega_o, \theta_o, \phi_o)} \quad . \tag{4.8}$$

This is the nomenclature used previously to phase the elements for a beam maximum in the direction $\theta_o\phi_o$, except $\Delta_{nm} = \psi_{nm}(\theta_o, \phi_o)$, $\eta_{nm} = \xi_{nm}(\theta_o, \phi_o)$. It must be emphasized that one does not calculate the radiation pattern with this approach. The phase angles are the same (after taking the conjugate of s^*_{nm}), but because of the added amplitude factor, the correlation pattern is somewhat different from the radiation pattern.

In the following sections, estimates will be given of the numbers of s_{nm} that are required, and of the speed possible in their generation or retrieval from storage. The reader should keep in mind that some combination of analog and digital techniques is required for these s^*_{nm} and ultimately for the R_{nm}. The question of implementation is deferred to Section 4.3.

4.2 System Requirements

4.2.1 Basic Assumptions.

In the following discussion it is assumed that:

1) Hemispherical coverage is necessary for any signal in the band 0.6 - 3.0 GHz.

2) All of the space and frequency domains should be searched in one second.

3) The overall array gain should be 20 db.

4) Angular resolution should be $\pm 1^o$. Accurate target location will be determined with the assistance of an auxiliary computer and at the discretion of the operator.

5) No discussion need be given of a tracking mode of operation at this time since this problem may not be of interest to the sponsor.

4.2.2 Basic Data Rates and Storage Requirements.

The data rates and storage requirements are dependent on three parameters: the number of elements (μ) in the array, the number of frequency increments (F), and the number of distinct angular pointing directions (N). With a specification of 20 db gain, and using spiral antennas, the number of elements, μ , can be fairly well determined from the far field calculations discussed in Chapter II of this and the previous report. From these studies, a first estimate is that at least 31 elements will be needed (to be contained in a cone of half angle 45^{o}) when 91 elements are placed on the entire hemisphere.

The number of frequency increments, F , must be determined by balancing the conflicting requirements that:

1a) The signal-to-noise ratio be kept high.

1b) The difference in frequency between incident and reference signals be kept small.

2a) The total sweep time be kept small.

2b) Sufficient bandwidth be provided for broadband signals.

From these requirements, a 1 MHz bandwidth has been arbitrarily specified, giving F= 3000 - 600 / 1 = 2400 increments.

If the beam is to be pointed at different discrete points, the number of such points, N, can be obtained by dividing the total hemisphere, of area 2π steradians, into N incremental areas. If the centers of these incremental areas are to be 2^{o} apart, the number of such areas is

$$\frac{2\pi}{(.65)(2)^{2}(\pi/180)^{2}} = 8000 \quad .$$

The factor .65 is obtained by assuming hexagonal incremental areas.

These values of F = 2400 and N = 8000 thus dictate a rate $M_1=FN$ of 19.2×10^6 different observations. If this were to be accomplished in one second, the clock rate would have to be 19.2 MHz, giving a time per observation rate of 52×10^{-9} seconds.

The severe limitation in this brute force approach is the enormous amount of data ($M_2=2\mu FN$) that must be stored or calculated. Since there are 91 elements, 182 values of P_{nm} and Q_{nm} must be specified at every observation point, even though many can be set equal to zero. Thus, for the 1^o case, there are $M_2=182 \times 19.2 \times 10^6=3.5 \times 10^9$ different 'words' of information (the number of bits in a digital system would be at least a factor of five or six higher if reasonable accuracy is to be maintained) that must be cycled through if the problem has to be handled sequentially. Fortunately, there is a good deal of redundancy as discussed in the next section.

4.2.3 Simplifications in the System Requirements.

The enormous numbers of required data that have been calculated in the previous section can be substantially reduced by taking advantage of redundancies in the expressions for s^*_{nm} and of symmetries in the element location on the sphere. These simplifications are discussed in the following order: 1) the number of elements, μ , 2) the number of frequency increments, F, and 3) the number of incremental areas that must be scanned, N .

The total number of elements, μ , is dictated by the specified gain (20 db in this case) and thus the tctal of 91 elements cannot be appreciably reduced. However, because the elements can be symmetrically located (using half of an icosahedron) on the hemisphere, two major simplifications can be utilized. Six separate regions can be conjointly or sequentially scanned around the six vertices of the half icosahedron. In addition, a five-fold symmetry exists around each vertex; mirror imaging increases this by another factor of two.

Thus the same s^*_{nm} information can be applied to 30 (and possibly 60) different sectors of the hemisphere. Two of these symmetrical sectors are shown in Fig.4-1, showing a top view of the hemisphere and the 91 element locations. It should be emphasized that this simplification is gained at the expense of added parallel circuitry or of switching networks.

The number of frequency increments, F, can be lowered by the simple expedient of increasing the IF bandwidth, say from 1 - 5 MHz. A more subtle approach is to parallel several 1 MHz bands, each using the same local oscillator frequency and the same s^*_{nm} . Phase errors will then exist; a computer test is planned to determine how many such bands can be handled at the same time without serious degradation of accuracy. It will be necessary to duplicate some,but not all , of the circuitry needed to calculate R, $\overline{R}$, etc , since the different bands can be carried on different carriers and the output display can certainly be used to display all signals at once.

An important reduction of the storage requirements for the s^*_{nm}, also related to F, can be obtained by noting that the definition of s^*_{nm} contains $k_q a$ in only one term so that the phase angle can be broken up into two parts as

$$\Phi_{nm}(\omega_q, \theta_r, \phi_s) = \Phi^{\ell}_{nm}(\omega_\ell, \theta_r, \phi_s) + q\,\delta\,\Phi_{nm}(\delta\omega, \theta_r, \phi_s) \qquad 4.9)$$

where

$$\Phi^{\ell}_{nm}(\omega_\ell, \theta_r, \phi_s) = k_\ell\, a\psi_{nm}(\theta_r, \phi_s) + \xi_{nm}(\theta_r, \phi_s) \qquad (4.10)$$

and

$$\delta\Phi_{nm}(\delta\omega, \theta_r, \phi_s) = \delta\, ka\psi_{nm}(\theta_r, \phi_s) \qquad (4.11)$$

with $k_\ell = \omega_\ell/c$, $\delta k = \delta\omega/c$; $f_\ell = \omega_\ell/2\pi$ is the lowest frequency of operation. The obvious advantage is that storage of s^*_{nm} for each frequency is not required; only the two values corresponding to the lowest and incremental values are needed.

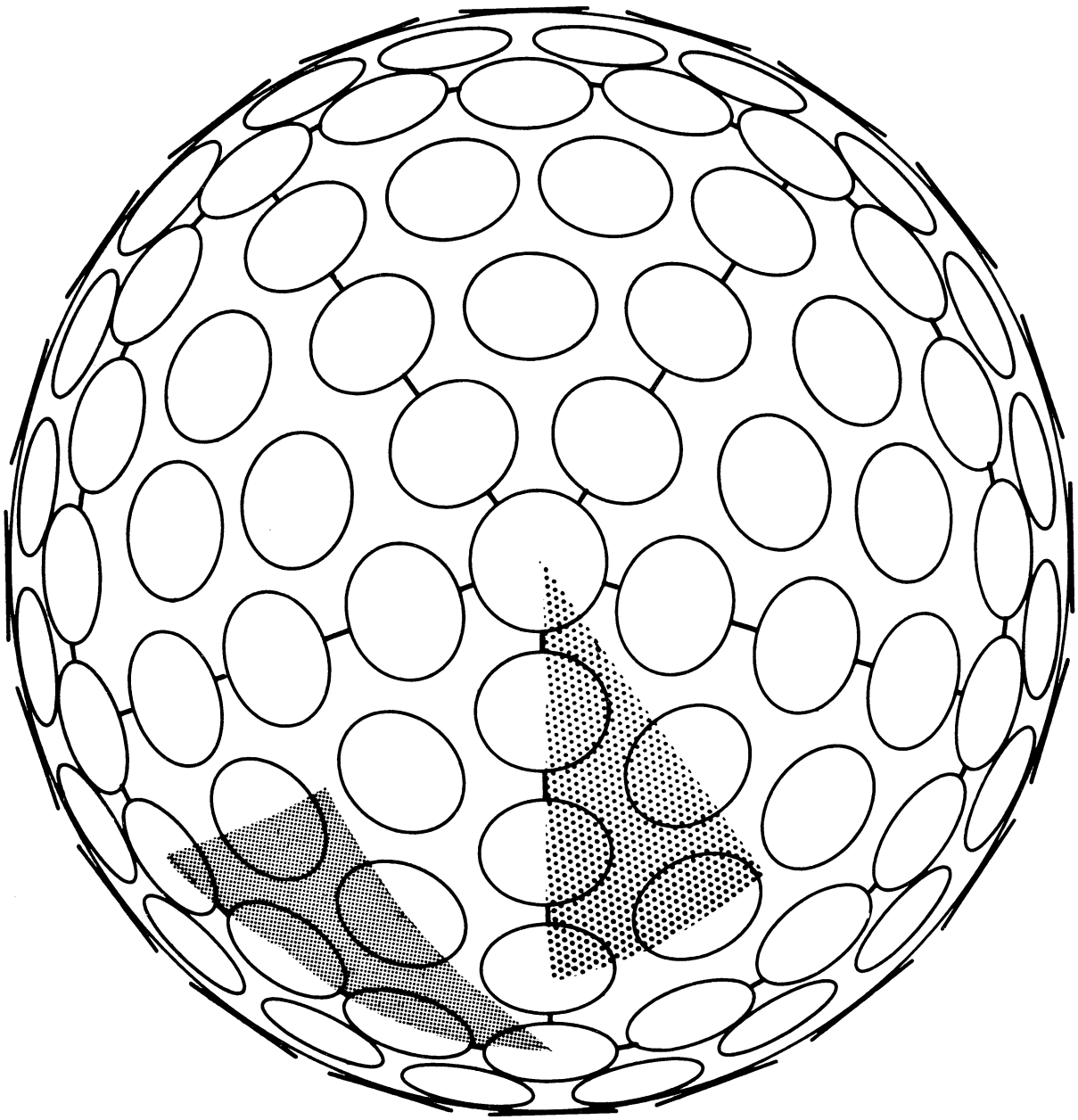

FIG. 4-1: SPHERICAL ARRAY - ELEMENT LOCATIONS AND SYMMETRICAL SECTORS.

The number of angular increments, N, can also be significantly reduced. First, is the obvious choice of increasing the angular interval. Since the minimum beamwidth for 31 elements is about 6^o, then an angular increment even as large as 6^o ($\pm$ 3^o) would still locate all sources. This would provide a factor of nine savings in storage requirements. The calculation of pointing direction might be somewhat degraded; this would be dependent on the location technique which will necessarily involve a separate computation anyway. Because of the larger beamwidths at lower frequencies, it is possible to effect a further reduction by relating the number of angular increments to the frequency. This would provide at most an additional factor of two savings at the expense of added instructional complexity.

By combining these techniques we see that the original estimate of the data rate (M_1) can be significantly reduced by processing five 1-MHz bands simultaneously ($F' = F/5$) and using six simultaneous beams with 6^o accuracy ($N' = 1/6\ (2^o/6^o)^2 N$). The new data rate is thus $M_1 = \frac{19.2\ \text{MHz}}{270} = 71$ KHz. The storage requirements (denoted now by double primes) for M_2 are reduced even more drastically. When six beams are employed only $\mu'' = 31$ different values of s^*_{nm} are required rather than 91. F'' can be reduced simply to 2 by taking advantage of the redundancy in frequency. Since $N''=N' = \frac{N}{54} = 148$, the storage requirements are now $M_2 = 2 \times 31 \times 2 \times 148 = 18,400$. Alternatively,

$$\frac{3.5 \times 10^9}{(91/31)(2400/2)(54)} = \frac{3.5 \times 10^9}{1.9 \times 10^5} = 18,400.$$

This number is quite modest and is achievable with numerous storage techniques.

4.3 Implementation

4.3.1 Survey of Techniques.

The description of the correlation process in the Second Quarterly made no mention of implementation, although an analog approach was implied. It now

appears that the costs and speeds of digital systems are entirely competitive . In the following, various combinations of analog and digital techniques will be discussed.

One assumption that should be repeated is that the accurate specification of angle will be made in an auxiliary mode. The present system is only to be capable of plotting the correlation pattern and of alerting the operator to the presence of a target which can then be located more accurately. It does not now seem advantageous to use the usual null technique for target location since the phasing requirements for a null must be determined empirically for each frequency and angle. Another possibility is to calculate the source location (possibly using phase information) from a set of values measured near the suspected source location. The optimum distance from the beam maximum could be determined from computer simulations. A third possibility is to create a 'wobbling' beam mode. Only when the beam is wobbling around the correct position would the response be steady in time. The extent of the cyclic variations would tell the operator how to move the center of the wobbling to minimize these variations.

The long time required to digitally compute the trigonometric functions contained in Φ_{nm} seems to preclude a digital computation of the s^*_{nm}. Time and expense considerations also suggest that the multiplication of x_{nm} and s^*_{nm} can best be performed by analog techniques. Thus, there are really only two possibilities; 1) that the values of s^*_{nm} (or at least the phase of s^*_{nm}) be stored in a computer memory and after retrieval, converted to an analog form for the calculation of R_{nm}, and 2) that the values of s^*_{nm} be generated by analog techniques. These two approaches are the subject of the following sections.

4.3.2 Computer Storage of s^*_{nm}

As previously described, perhaps only 18,400 different values of s^*_{nm} need

be specified, regardless of the number of frequency increments F' that are assumed. This data might be obtained through 31 transducers on a magnetic disk or drum, each feeding a number of antennas the values of s^*_{nm}. Due to the relatively slow rotation (1800 rpm), several frequency bands would have to be computed in one revolution of the disk or drum so that all bands could be searched in one second. Using the technique: $\Phi = \Phi^{\ell} + \delta\Phi$, it will be necessary to have an intermediate storage that stores the values of Φ as they are generated. Possibly, this could be done without a rotating storage device. In a preliminary study, it would be proper to feed all data in sequentially, so that only one reading head need be employed.

The reduction in storage requirements described in the previous section was obtained largely by taking advantage of the redundancy in phase information as a function of frequency. Unfortunately, the quantity Φ occurs as an exponential and can be easily incremented only with phase modulated amplifiers. This suggests a combined digital-analog approach; the digitally stored values of Φ_{ℓ} and $\delta\Phi$ can be used to generate Φ which is used to phase modulate a carrier frequency.

In an entirely digital technique, the real and imaginary parts must be calculated and temporarily stored for use at the next frequency. Thus,

$$e^{-j\Phi_{nm}(q,r,s)} = \cos\left[\Phi_{nm}(q-1,r,s)+\delta\Phi_{nm}(r,s)\right] - j\sin\left[\Phi_{nm}(q-1,r,s)+\delta\Phi_{nm}(r,s)\right] \tag{4.12}$$

and thus

$$\cos\Phi_{nm}(q,r,s) = A_{nm}(r,s)\cos\Phi_{nm}(q-1,r,s) - B_{nm}(r,s)\sin\Phi_{nm}(q-1,r,s) \tag{4.13}$$

$$\sin \Phi_{nm}(q,r,s)=A_{nm}(r,s)\sin \Phi_{nm}(q-1,r,s)+B_{nm}(r,s)\cos \Phi_{nm}(q-1,r,s) \quad , \quad (4.14)$$

where

$$A_{nm}(r,s)=\cos \delta \Phi_{nm}(r,s); \; B_{nm}(r,s)=\sin \delta \Phi_{nm}(r,s) \quad .$$

Whether the saving in storage requirements justifies the added circuitry needed to obtain the values of $\cos \Phi_{nm}(q,r,s)$ and $\sin \Phi_{nm}(q,r,s)$ will have to be ascertained after more study. The important thing is apparently whether circuitry can be developed which performs this computation rapidly enough. If this is the case, then the storage requirements can perhaps be sufficiently reduced to justify a non-rotating and more rapid access memory for each of the 31 different elements.

Storage devices presently available can satisfy the requirements even without taking advantage of the redundancy in frequency if several of the other simplifications are employed. Thus if the basic storage requirements discussed in Section 4.2.1 are reduced by a factor of 300 by some combination of μ'', F'' and N'', then roughly 10×10^6 words need be stored. If each word contained six bits, this could be handled by a single disk (which has a maximum capacity of 65 million bits). Also, recent developments in batch fabricated ferrite memories indicate capacities of a quarter million bits in a 4" cube, with total capacities of 10^8 bits at a cost of 0.1 cents per bit, including electronics. A typical access rate for disks (used as a serial output device, i.e. no random access) and for conventional magnetic core memories is approximately 1 MHz.

Magnetic core memories are available using special read-out techniques, which operate at a 5 MHz rate and provide random access as well. Magnetic film techniques also appear to provide the required speed, though costs are high due to the more expensive associated circuitry. However, with the rapid development in memory techniques it seems very probable that the cost aspect will not be a major problem.

Prior to obtaining R_{nm}, and $\overline{R}_{nm}$, P and Q must be stored for each of the antenna elements being processed. For this storage however, silicon micro-circuit flip-flops would be used. Since operating speeds of up to 40 MHz are available, no computation rate problems are anticipated.

4.3.3 Analog Generation of s^*_{nm}

In an analog approach there are essentially two ways to scan over the hemisphere or sections of the hemisphere: 1) a 'spiral' scan in which ϕ is varied most rapidly, or 2) an 'oscillating' scan in which θ is varied most rapidly. In either case we can describe the beam maximum position as

$$\theta = g_1(t), \qquad \phi = g_2(t)$$

and in a simple case, we might have

$$\cos\theta = \cos\omega_1 t \qquad \cos\phi = \cos\omega_2 t \quad .$$

In the generation of the terms needed in specifying ψ_{nm} given by (4.4), it is possible to avoid phase shifters and multipliers by using such trigonometric identities as

$$\cos(\phi-\beta_{nm}) = \cos\phi\cos\beta_{nm} + \sin\phi\sin\beta_{nm} = C_{nm}\cos\phi + S_{nm}\sin\phi$$

$$\sin\theta\cos\phi = \frac{1}{2}\sin(\theta+\phi) + \frac{1}{2}\cos(\theta-\phi) \quad .$$

By this means ψ_{nm} can be obtained for each element by the addition of four signals of appropriate amplitude (frequencies f_1, f_2, f_1+f_2, f_1-f_2). These values of ψ would have to be multiplied by ka; presumably by amplification proportional to time, since the local oscillator frequency is presumed to be changing linearly.

A more difficult problem is the generation of the terms ξ_{nm} given by (4.5) which account for the different polarizations seen at each element and for the

differing orientations of the different elements. Since

$$c+jd=\sqrt{c^2+d^2}\; e^{j\tan^{-1}\left[\frac{d}{c}\right]},$$

then it can be shown that

$$e^{j\xi_{nm}} = \frac{1}{1+\cos\gamma_{nm}}\left[\sin\alpha_n\sin\theta+(\cos\alpha_n\cos\theta+1)\cos(\phi-\beta_{nm})\right.$$

$$\left.+j(\cos\alpha_n+\cos\theta)\sin(\phi-\beta_{nm})\right]. \qquad (4.15)$$

In an analog scheme, it would be difficult to include the first factor $(1+\cos\gamma_{nm})^{-1}$, which varies between 1 and 2. It is therefore likely that this amplitude factor should be ignored. The generation of the other two terms would proceed as before and the amplitude weighting applied to components of the carrier which are 90^o out of phase (thereby taking account of j) will change the phase in the desired manner. The decomposition into four signals will again allow their generation without multipliers.

In summary, for the analog approach: an approximate value for the function $s^*_{nm}(\omega, \theta, \phi)$ may be obtained from the proper combination of four signals with frequencies f_1, f_2, f_1+f_2, f_1-f_2 without the necessity of analog multipliers. The disadvantage of this scheme is the complexity of generating all the signals. It does seem to offer the possibility for fairly rapid scan, since we can have a total scan time of one second with an IF bandwidth of 1 MHz (giving F=2400) and a frequency f_2 of 2400 KHz (varying ϕ) and $f_1 = \frac{360^o}{3^o} \times 2400 = 288$ KHz. It might also be mentioned that some of these analog techniques might be useful in a digital approach, thereby taking advantage of redundancy in angular information.

V

EXPERIMENTAL WORK

Currently, flat spiral antennas are being evaluated as possible antenna elements of the spherical array. During the present period we have experimentally studied two spiral antenna configurations. One of these is a commercial antenna which operates in the frequency range 1 - 11 GHz. The other antenna is an Archimedean spiral designed and fabricated at the Radiation Laboratory. This antenna was designed to operate from 600 MHz to 3000 MHz. VSWR characteristics of these two antennas have been measured and found to be less than 3:1 over their design frequencies of operation. The patterns produced by the spirals have been measured in the free-space environment. Figures 5-1 and 5-2 show the patterns of the spiral antenna built at The University of Michigan Radiation Laboratory.

To assist in the theoretical work, a hemispherical mold has been fabricated, from which a fiberglass shell having a diameter of 6' will be fabricated and metallized. Sixteen spiral antennas will be arranged over the surface of the shell from which experimental data will be obtained. The spiral antennas to be used are of the type designed by the Radiation Laboratory. These antennas will be mounted on the hemisphere as follows: one at the north pole, five located symmetrically around the north pole at $\theta = 15^{o}$ and an additional 10 located symmetrically around the north pole at $\theta = 30^{o}$. The 16 antennas will be fed by a 16-way stripline power divider similar in construction to the 8-way power divider described in the Second Quarterly Report.

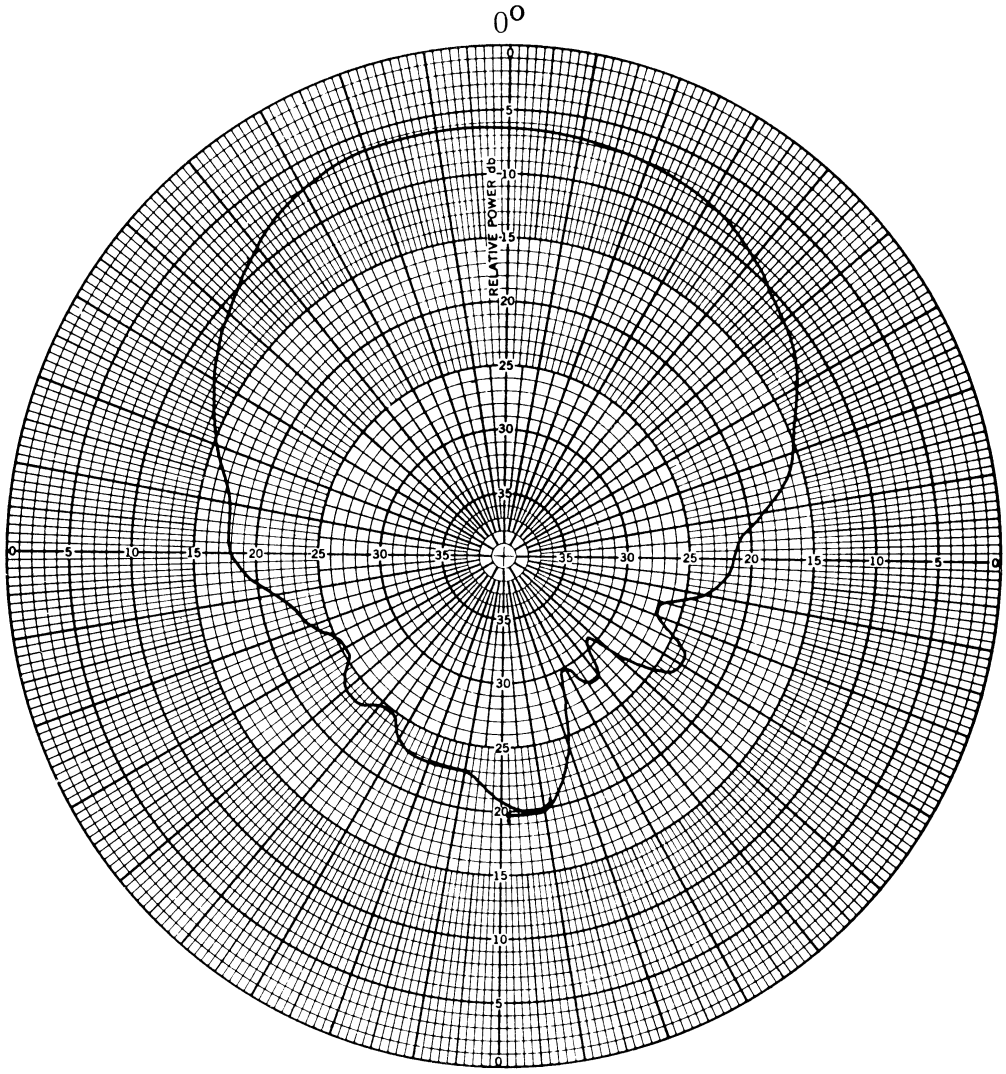

FIG. 5-1: FLAT SPIRAL E-PLANE PATTERN
2.15 MHz.

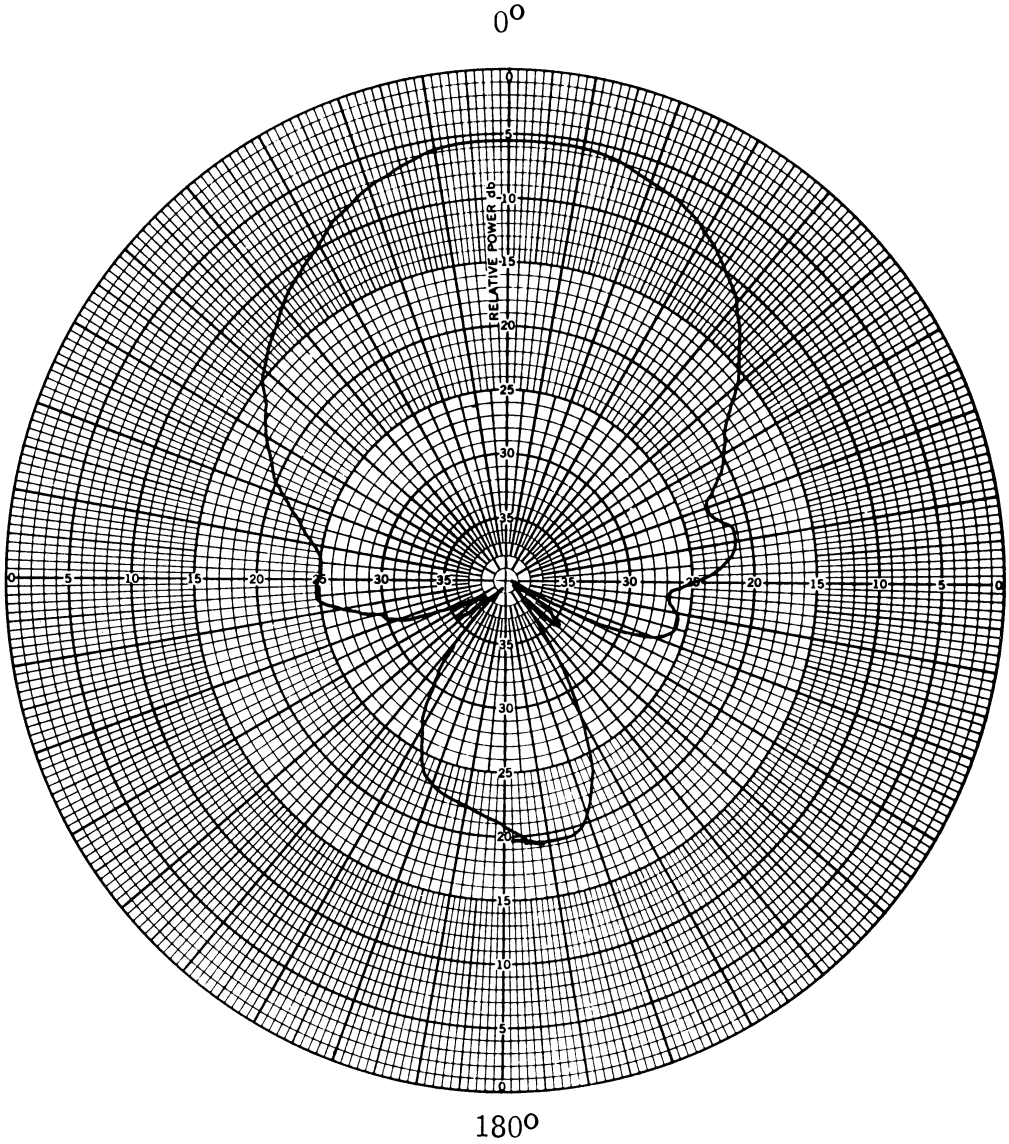

FIG. 5-2: FLAT SPIRAL H-PLANE PATTERN
2.15 MHz.

VI

REFERENCES

Sengupta, D. L., J. E. Ferris, R. W. Larson and T. M. Smith (1965), "Azimuth and Elevation Direction Finder Study," Quarterly Report No. 1, ECOM-01499-1, The University of Michigan Radiation Laboratory Report 7577-1-Q.

Sengupta, D. L., J. E. Ferris, G. Hok, R. W. Larson and T. M. Smith (1966), "Azimuth and Elevation Direction Finder Study," Quarterly Report No. 2, ECOM-01499-2, The University of Michigan Radiation Laboratory Report 7577-2-Q.

Silver, S. (1949), Microwave Antenna Theory and Design, McGraw-Hill Book Company, Inc., New York, pp. 192-195.

Smith, T. M. (1966), "An Approximation of a Spherical Array by a Continuous Field Distribution in a Spherical Aperture," The University of Michigan Radiation Laboratory Internal Memorandum, 07577-511-M.

THE UNIVERSITY OF MICHIGAN

DISTRIBUTION LIST FOR 07577 QUARTERLY REPORTS

Address	No. of Copies
Mr. E. M. Turner AVWE-3 Air Force Avionics Laboratory Wright-Patterson AFB, Ohio 45433	1
Mr. C. J. Sletten CRD Air Force Cambridge Research Laboratories L. G. Hanscom Field Bedford, Massachusetts 01731	1
Mr. C. L. Pankiewicz EMATA Rome Air Development Center Griffiss AFB, New York 13442	1
Mr. P. A. Lantz, Code 525 NASA Goddard Space Flight Center Greenbelt, Maryland 20771	1
USAEL Liaison Officer RAOL Rome Air Development Center Griffiss AFB, New York 13442	1
Mr. J. B. Norvell, R31 National Security Agency Ft. G. G. Meade, Maryland 20755	1
Mr. R. J Adams Code 5330 Naval Research Laboratory Washington, D. C. 20390	1
Mr. R. Fratila Code 362A Dept of the Navy, BuShips Main Navy Building Washington, D. C. 20360	1
U. S. Army Electronics Command AMSEL-HL-R Ft. Monmouth, N J. 07703	1
Mr. B. I Small, Code 3220C U. S. Navy Electronics Laboratory San Diego, California 92152	1
Harry Diamond Laboratories Technical Library Connecticut Ave., and Van Ness St., NW Washington, D. C. 20438	1

Mr. C. Craig IALOG/ESE U. S. Army Security Agency Arlington Hall Station Arlington, Virginia 22207	1
U. S. Army Electronics Command AMSEL-NL-R Ft. Monmouth, N. J. 07703	1
Defense Documentation Center DDC-IRE Cameron Station, Building 5 Alexandria, Virginia 22314	20 + card
Office, Assistant Secretary of Defense Research and Engineering Technical Library, Pentagon Room 3E1065 Washington, D. C. 20301	1
Defense Intelligence Agency DIARD Washington, D. C. 20301	1
Department of the Navy BuShips Technical Library Code 312, Room 1528 Main Navy Building Washington D C 20325	1
U. S. Naval Research Laboratory Code 2027 Washington, D. C. 20390	1
U. S. Navy Electronics Laboratory Technical Library San Diego, California 92101	1
AFSC Scientific and Technical Liaison Officer RTSND U S Naval Air Development Center Johnsville, Warminster, Pennsylvania 18974	1
Systems Engineering Group SEPIR Wright-Patterson AFB, Ohio 45433	1
ESD, AFSC, Scientific/Technical Information Div. (ESTI) L. G. Hanscom Field Bedford, Massachusetts 01731	2

Air Force Cambridge Research Laboratories
CRXL-R
L. G. Hanscom Field
Bedford, Mass 01731 2

NASA Repr. Scientific and Technical Information Facility
P O Box 5700
Bethesda, Md 20014 1

U. S. Army Electronics Command
AMSEL-WL-S
Ft. Monmouth, N. J. 07703 5

U. S. Army Electronics Command
EW-MET Commodity
AMSEL-EW, Management Office
Ft. Monmouth, N. J. 07703 1

U. S. Army Electronics Command
AMSEL-MR
225 S. 18th St.
Philadelphia Pa 19103 1

U. S. Army Electronics Command
AMSEL-IO-T 1

AMSEL-XL-D 1

AMSEL-RD-MAT 1

AMSEL-RD-MAF 1

AMSEL-RD-LNA 1

AMSEL-RD-LNR 1
Ft. Monmouth, N. J. 07703

U. S. Army Electronics Command
R and D Activity
White Sands Missile Range, New Mexico 88002 1

U. S. Army Electronics Command
Mountain View Office - Electronic Warfare Laboratory
Box 205
Mountain View, California 1

U. S. Army Engineer R and D Laboratories
STINFO Branch
Ft. Belvoir, Va. 22060 1

U. S. Army Electronics Command Intelligence Materiel Development Office Electronic Warfare Laboratory Fort Holabird, Md. 21219	1
U. S. Army Electronics Command ASDL-9 Liaison Officer Aeronautical Systems Division Wright-Patterson AFB, Ohio 45433	1
U. S. Army Electronics Command Liaison Officer EMPL Rome Air Development Center Griffiss AFB, New York 13442	1
US NBS Boulder Laboratories Technical Library Boulder, Colorado 80301	1
Department of the Army Chief, Research and Development Washington, D C 20315	2
Department of the Army Chief, Communications-Electronics CCEES-1A Washington, D C. 20315	1
U. S. Army Materiel Command R and D Directorate Washington, D. C 20315	2
U. S. Army S A S O C 52D Fort Huachuca, Ariz. 85613	1
U. S. Army Combat Developments Command Communications-Electronics Agency Fort Huachuca, Ariz. 85613	1
U. S Army Electronic Proving Ground Technical Library Fort Huachuca, Ariz. 85613	1
U. S. Army Security Agency AC of S, G4 (Technical Library) Arlington Hall Station Arlington, Va. 22207	2
Total List	75

UNCLASSIFIED

Security Classification

DOCUMENT CONTROL DATA - R&D

(Security classification of title, body of abstract and indexing annotation must be entered when the overall report is classified)

1. ORIGINATING ACTIVITY *(Corporate author)*
The University of Michigan Radiation Laboratory
Department of Electrical Engineering
Ann Arbor, Michigan 48108

2a. REPORT SECURITY CLASSIFICATION
UNCLASSIFIED

2b. GROUP

3. REPORT TITLE
Azimuth and Elevation Direction Finder Study

4. DESCRIPTIVE NOTES *(Type of report and inclusive dates)*
Third Quarterly Report 1 March - 31 May 1966

5. AUTHOR(S) *(Last name, first name, initial)*
Sengupta, Dipak L.; Ferris, Joseph E.; Hok, Gunnar; Larson, Ronal W. and Smith, Thomas M.

6. REPORT DATE	7a. TOTAL NO. OF PAGES	7b. NO. OF REFS
15 June 1966	37	4

8a. CONTRACT OR GRANT NO.	9a. ORIGINATOR'S REPORT NUMBER(S)
DA 28-043 AMC-01499(E)	7577-3-Q
b. PROJECT NO. 5A6 79191 D902 01 04	
c.	9b. OTHER REPORT NO(S) *(Any other numbers that may be assigned this report)*
d.	ECOM-01499-3

10. AVAILABILITY/LIMITATION NOTICES

Each transmittal of this document outside the Department of Defense must have prior approval of USAECOM, AMSEL-WL-S, Ft. Monmouth, N. J. 07703.

11. SUPPLEMENTARY NOTES	12. SPONSORING MILITARY ACTIVITY
	U. S. Army Electronics Command AMSEL-WL-S Fort Monmouth, New Jersey 07703

13. ABSTRACT

Radiation properties of a spherical antenna array are discussed. The array consists of circularly polarized antenna elements arranged according to a predetermined fashion on a spherical surface. The variation of the radiation patterns, directivity and the half-power beamwidths of the patterns with the change of different parameters of the array are discussed. A simple approximate (but useful) expression is given which can be used to analyze the patterns produced by a spherical array. Subsidiary lobes in the pattern produced by circular arrays of isotropic elements are discussed.

A technique of correlation processing of the output data from each antenna element of the array for direction finding purposes is described.

Experimental patterns produced by a flat spiral antenna are given.

DD FORM 1 JAN 64 1473

UNCLASSIFIED

Security Classification

14. KEY WORDS	LINK A		LINK B		LINK C	
	ROLE	WT	ROLE	WT	ROLE	WT
ANTENNA ARRAY SPHERICAL ARRAY CIRCULAR ARRAY GRATING LOBES DATA PROCESSING ARRAY FLAT SPIRALS						

INSTRUCTIONS

1. ORIGINATING ACTIVITY: Enter the name and address of the contractor, subcontractor, grantee, Department of Defense activity or other organization *(corporate author)* issuing the report.

2*a*. REPORT SECURITY CLASSIFICATION: Enter the overall security classification of the report. Indicate whether "Restricted Data" is included. Marking is to be in accordance with appropriate security regulations.

2*b*. GROUP: Automatic downgrading is specified in DoD Directive 5200.10 and Armed Forces Industrial Manual. Enter the group number. Also, when applicable, show that optional markings have been used for Group 3 and Group 4 as authorized.

3. REPORT TITLE: Enter the complete report title in all capital letters. Titles in all cases should be unclassified. If a meaningful title cannot be selected without classification, show title classification in all capitals in parenthesis immediately following the title.

4. DESCRIPTIVE NOTES: If appropriate, enter the type of report, e.g., interim, progress, summary, annual, or final. Give the inclusive dates when a specific reporting period is covered.

5. AUTHOR(S): Enter the name(s) of author(s) as shown on or in the report. Enter last name, first name, middle initial. If military, show rank and branch of service. The name of the principal author is an absolute minimum requirement.

6. REPORT DATE: Enter the date of the report as day, month, year; or month, year. If more than one date appears on the report, use date of publication.

7*a*. TOTAL NUMBER OF PAGES: The total page count should follow normal pagination procedures, i.e., enter the number of pages containing information.

7*b*. NUMBER OF REFERENCES: Enter the total number of references cited in the report.

8*a*. CONTRACT OR GRANT NUMBER: If appropriate, enter the applicable number of the contract or grant under which the report was written.

8*b*, 8*c*, & 8*d*. PROJECT NUMBER: Enter the appropriate military department identification, such as project number, subproject number, system numbers, task number, etc.

9*a*. ORIGINATOR'S REPORT NUMBER(S): Enter the official report number by which the document will be identified and controlled by the originating activity. This number must be unique to this report.

9*b*. OTHER REPORT NUMBER(S): If the report has been assigned any other report numbers *(either by the originator or by the sponsor)*, also enter this number(s).

10. AVAILABILITY/LIMITATION NOTICES: Enter any limitations on further dissemination of the report, other than those imposed by security classification, using standard statements such as:

(1) "Qualified requesters may obtain copies of this report from DDC."

(2) "Foreign announcement and dissemination of this report by DDC is not authorized."

(3) "U. S. Government agencies may obtain copies of this report directly from DDC. Other qualified DDC users shall request through

_____."

(4) "U. S. military agencies may obtain copies of this report directly from DDC. Other qualified users shall request through

_____."

(5) "All distribution of this report is controlled. Qualified DDC users shall request through

_____."

If the report has been furnished to the Office of Technical Services, Department of Commerce, for sale to the public, indicate this fact and enter the price, if known.

11. SUPPLEMENTARY NOTES: Use for additional explanatory notes.

12. SPONSORING MILITARY ACTIVITY: Enter the name of the departmental project office or laboratory sponsoring *(paying for)* the research and development. Include address.

13. ABSTRACT: Enter an abstract giving a brief and factual summary of the document indicative of the report, even though it may also appear elsewhere in the body of the technical report. If additional space is required, a continuation sheet shall be attached.

It is highly desirable that the abstract of classified reports be unclassified. Each paragraph of the abstract shall end with an indication of the military security classification of the information in the paragraph, represented as *(TS), (S), (C), or (U)*.

There is no limitation on the length of the abstract. However, the suggested length is from 150 to 225 words.

14. KEY WORDS: Key words are technically meaningful terms or short phrases that characterize a report and may be used as index entries for cataloging the report. Key words must be selected so that no security classification is required. Identifiers, such as equipment model designation, trade name, military project code name, geographic location, may be used as key words but will be followed by an indication of technical context. The assignment of links, rules, and weights is optional.